



MODELING OF BASE ISOLATED NUCLEAR POWER PLANT SUBJECTED TO BEYOND DESIGN BASIS SHAKING

Gilberto Mosqueda¹, Joaquin Marquez², Patrick Hughes²

¹ Professor, Structural Engineering, University of California, San Diego, USA

² Graduate Student, Structural Engineering, University of California, San Diego, USA

ABSTRACT

Modeling of the seismic isolation system plays a key role in simulating the seismic response of base isolated nuclear power plants (NPPs), including estimation of peak isolator displacement and potential to exceed the clearance to stop. Under beyond design basis shaking, seismic isolators are expected to undergo large displacements and exhibit complex behaviour. Developing accurate models of lead rubber bearings (LRB) proposed for use in NPPs, can be challenging due to the nonlinear effects of the cyclic heating causing strength degradation and strain hardening in the rubber at large strains. A new modeling approach is proposed for simulating the cyclic behavior of LRB that aims to capture measured experimental data from full-scale bearings designed for NPPs that display these complex characteristics. The bearing models are then applied to determine estimates of displacement and potential impact velocity to a stop or moat wall, and to identify bearing characteristic that influence the overall response of the isolated structure. In order to consider the effects of impact to a stop, a moat wall or concrete retaining wall with backfill soil is considered in the model. The impact model is rooted in experimental data and high-fidelity Finite Element Simulations (FEM) to capture the impact force, contact duration, and deformation of the wall. The simulation tools being developed can be used to predict the consequences of bearing modeling and impact on the seismic performance of NPP and develop effective mitigation measures to reduce the risk under beyond design basis shaking.

INTRODUCTION

Seismic isolation is an effective strategy to protect critical facilities, including Nuclear Power Plants (NPPs), from the damaging effects of horizontal earthquake ground shaking. The increased flexibility and resulting elongation of the natural vibration period of the structure leads to significant reductions in forces transmitted to the structure above the isolation level, at the expense of large displacements in the isolation system hardware. The seismic isolation system needs to be designed to accommodate these displacements and have the necessary horizontal clearance or moat at the basement level. The clearance is often limited by a moat wall that can also function as a stop to limit displacement and thus prevent failure of the isolation system.

The modeling of the seismic isolation system also plays a key role in simulating the seismic response of NPPs including impact. Previous moat wall impact studies have found that impact velocity is a key factor into the severity of impact and is greatly influenced by the model used for seismic isolation (Sarebanha and Mosqueda 2017). Impact is expected to occur at very large displacement, at which point the behavior of the bearings can be complex. Developing accurate models of lead rubber bearings (LRB) has been challenging due to the nonlinear effects of the cyclic heating causing strength degradation and strain hardening in the rubber at large strains. A new modeling approach is proposed for simulating the behavior of LRB that aims to capture measured experimental data from testing of full-scale bearings. These models are then applied to determine estimates of displacement and potential impact velocity of isolated NPPs when considering the complex bearing behavior.

In NPPs, moat wall impact is of significant concern due to the potential for increased transfer of forces and amplification in response of the structural system, piping and other sensitive contents. However, neither the consequences of impact nor the factors important to mitigate its effects are well understood. The objectives of this study are to examine the effects of impact on the response of seismically isolated NPPs and identify characteristics of the isolation hardware and hard stop that minimize these effects. In this study, modeling of moat wall impact as applied to a model of the APR1400 in previous studies is revisited (Sarebanha and Mosqueda 2017). In particular, high-fidelity Finite Element Simulations (FEM) are examined as a means of verification of moat wall models subjected to impact. To first gain confidence in the FEM tools, experimental data on large scale structural impact experiments was examined and FEM simulations were conducted to replicate the observed impact behavior. These studies are on-going with two sets of data from ¼ scale experiments and full-scale experiments simulating a building impacting a moat wall. The insight gained from these studies will be used to build a detailed FEM model to simulate impact forces for an archetype NPP.

The combined improvement in modeling of bearings and moat wall impact provide advanced simulation tools for examining the seismic behavior of NPP under extreme earthquakes. The simulation tools can be used to predict the consequences of impact in the NPP and develop effective mitigation measures to reduce the risk of impact.

PARALLEL NUMERICAL BEARING MODELS

In an effort to develop reliable bearing models that are able to capture the behavioral characteristics of lead-rubber bearings under large amplitude cyclic displacements, elastomeric bearing models available in OpenSees (McKenna et al. 2000) are first reviewed. While certain models capture key characteristics, a model demonstrating the capacity to capture the full complex responses of LRBs has not yet been implemented. Characteristics of particular interest include the strength reduction in the bearing due to the heating of the lead core as well as hardening at high strains. To remedy extant deficiencies, it will be demonstrated that a combination of parallel models can be an effective approach to achieve adequate results that reflects actual bearing behavior. A summary of each element will be discussed, as well as the combinations of the models that were utilized to capture behavior observed in experimental data for large bearings. In order to evaluate the responses of the different models under earthquake excitation, a model of a nuclear power plant is subsequently examined in the following chapter.

LeadRubberX Element

In order to capture both the strength reduction in the bearing due to the heating of the lead and the hardening due to high strains, two models were combined in parallel. The OpenSees model used to capture the lead heating effect in the parallel model is LeadRubberX (LRX). This coupled bi-directional model's hysteresis is isotropic in nature due to the degradation of the hysteresis (i.e. the characteristic strength of the lead). In the equations shown below, the forces F_x and F_y are in terms of displacements U_x and U_y , along orthogonal directions x and y, respectively, are (Kalpakidis and Constantinou 2009):

$$\begin{Bmatrix} F_x \\ F_y \end{Bmatrix} = c_d \cdot \begin{Bmatrix} \dot{U}_x \\ \dot{U}_y \end{Bmatrix} + K_2 \cdot \begin{Bmatrix} U_x \\ U_y \end{Bmatrix} + (\sigma_{YL}(T_L)A_L) \cdot \begin{Bmatrix} Z_x \\ Z_y \end{Bmatrix} \quad (1)$$

$$Y \cdot \begin{Bmatrix} \dot{Z}_x \\ \dot{Z}_y \end{Bmatrix} = (A \cdot [I] - B \cdot [\Omega]) \cdot \begin{Bmatrix} \dot{U}_x \\ \dot{U}_y \end{Bmatrix} \quad (2)$$

$$[\Omega] = \begin{cases} Z_x^2 \cdot [sgn(\dot{U}_x Z_x) + 1] & Z_x Z_y \cdot [sgn(\dot{U}_y Z_y) + 1] \\ Z_x Z_y \cdot [sgn(\dot{U}_x Z_x) + 1] & Z_y^2 \cdot [sgn(\dot{U}_y Z_y) + 1] \end{cases} \quad (3)$$

In Equations 1-3, the overdot denotes differentiation with respect to time, $[I]$ is the identity matrix and dimensionless parameters Z_x and Z_y , are bounded by the values of ± 1 . The quantities A and B should be related with the following expression ($A=2B$), in order for the equations to properly function. Typically, A is set to 1 and B set equal to 0.5. These equations produce a typical hysteretic response of a smooth bilinear Bouc-Wen model but with a varying change in the yield strength of the lead, $\sigma_{YL}(T_L)$, as a function of the temperature of the lead (Kalpakidis and Constantinou 2009).

Bouc-Wen (Hardening) Element

The second element in the parallel system that can capture the hardening of the LRB at high strains is the *Bouc-Wen Bearing* model as implemented in OpenSees. This element utilizes the well-known Bouc-Wen model and enhances its capability to account for high strain hardening (Bouc 1967, Wen 1976). The enhancement that was incorporated into the model is Prager's rule. This phenomenological model was introduced for bearings by Casciati (Casciati 1989).

Along with the hardening capability, the model's hysteresis loops allow for rounded corners, which resemble the physical behavior of elastomeric bearings as described by Casciati. Casciati advanced the classical plasticity theory for bearing behavior by connecting the discontinuity between the elastic and plastic phases. The hardening effects increases as the displacement increases. The restoring force formulation also reaffirms that the model can be highly nonlinear depending on the value of μ in Eq. 4. If the value of μ is set high, then the hardening can occur prematurely, if it is set low then the hardening will occur at higher strains.

$$\begin{Bmatrix} F_x \\ F_y \end{Bmatrix} = K_2 \cdot \begin{Bmatrix} U_x \\ U_y \end{Bmatrix} + (\sigma_{YL} \cdot A_L) \cdot \begin{Bmatrix} Z_x \\ Z_y \end{Bmatrix} + K_3 \cdot \text{sgn} \begin{Bmatrix} U_x \\ U_y \end{Bmatrix} \cdot \begin{vmatrix} U_x^\mu \\ U_y^\mu \end{vmatrix} \quad (4)$$

$$K_3 = \alpha_2 \cdot K_{initial} \quad (5)$$

In Eq. 4, the first two terms in the restoring force formulation consists of post yield stiffness and the constant characteristic strength resembling that of a typical Bouc-Wen model. The model deviates with the last term of the equation, in which the hardening term is aggregated. Like the Bouc-Wen model, K_2 , is the linear post-yield stiffness. The parameter, α_2 , is the post-yield stiffness ratio of non-linear hardening component and therefore K_3 is the post-yield nonlinear stiffness.

HDR Element

The HDR model consists of an elastic component and a hysteretic component (Grant et al. 2004). The elastic component uses the Mooney-Rivlin strain energy function, with five elasticity constants. The hysteretic component uses an approach that is similar to bounding surface plasticity (Dafalias and Popov, 1975). As an improvement to the model by Huang and Fenves (2002), it provides a continuous response under load reversals without restrictions to harmonic loading. The formulation and details can be found in Grant et al. (2004).

Calibration of Parallel System (H-H-HDR Model)

A parallel system consisting of the three element models including LeadRubberX, Bouc-Wen, and HDR, is proposed and named H-H-HDR (Figure 1). The LeadrubberX element accounts for the heating of the lead and post elastic stiffness contribution from the rubber, the Bouc-Wen (hardening) element account for the hardening effect at higher strains, and HDR account for the 'Bauschinger' effect that are also seen at higher strains.

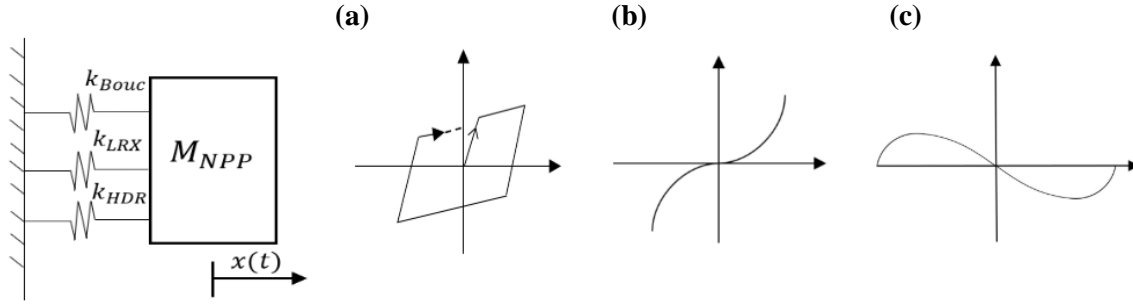


Figure 1. Parallel System. (a) LeadRubberX Element, (b) Bouc-Wen (hardening) Element, (c) HDR element

In order to calibrate model parameters based on the available experimental data, the initial design values from the manufacturer were first set as preliminary parameters. The `fminsearch` function in MATLAB was utilized to perform the calibration. The error measure used was the Normalized Root Mean-Squared Error (NRMSE) calculated using the difference of the experimentally measured force and the numerical force determined numerically using OpenSees and normalizing by the range of the maximum and minimum forces of the experiment. A multi-objective approach was undertaken to obtain a set of parameters for the selected calibration tests covering a range of strain and strain rates. Per Equation 7, all tests are considered when minimizing the objective function with equal weights assigned to each experiment considered. This calibration was conducted for select 1D tests listed in Table 1. The NRMSE results are also shown and contributions of the model components for test 15 can be seen in Figure 2.

$$\epsilon = \sum_{i=1}^{\text{no. tests}} (w_i \text{NRMSE}_i) \quad (7)$$

Table 1 NRMSE for Experimental Tests (H-H-HDR).

Test (#)	Strain (%)	Type	NRMSE (%)
14	100	1-D	5.95
8	200	1-D (GM)	6.04
11	300	1-D	4.25
13	400	1-D	3.81
15	500	1-D	2.83

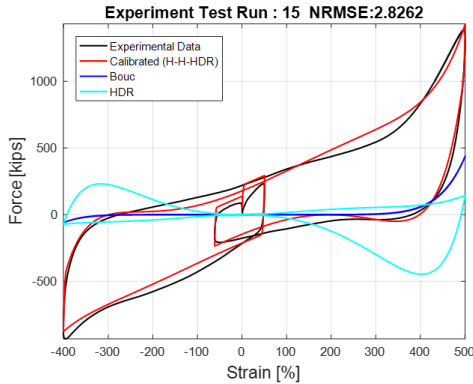


Figure 2. Calibration of Test 15 and Parallel System Contributions.

The calibrated bearing models were implemented in the APR 1400 ANT (Archetype Nuclear Test) model of a Nuclear Power Plant (NPP) to conduct simulations under 1D seismic excitation. The reader is referred to previous studies that have been conducted on the ANT model varying from hybrid testing considering experimentally measured bearing behavior (Zhao et al. 2015), sensitivity studies (Schellenberg et al. 2015), and moat wall impact studies (Sarebanha 2018). In order to assess the results obtained using the H-H-HDR model, peak bearing displacements and velocities at selected distances were compared to bilinear models considering strength degradation (LRX heating model) and a Bilinear model with constant strength. As shown in Figure 4, the average impact velocity at different shear strains and subsequent impacts are compared between the models. The H-H-HDR is essentially bounded by the upper and lower bounds models previously mentioned.

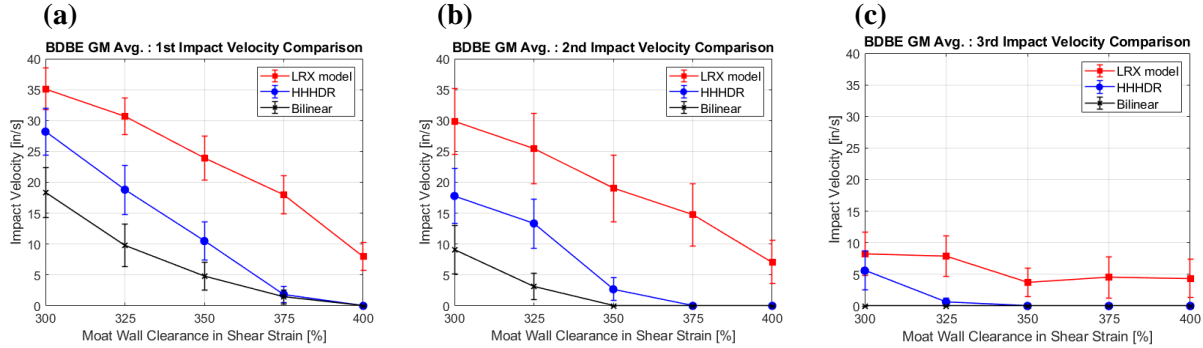


Figure 3. Avg. Impact Velocity vs Moat wall clearance: (a) 1st impact, (b) 2nd impact, (c) 3rd impact.

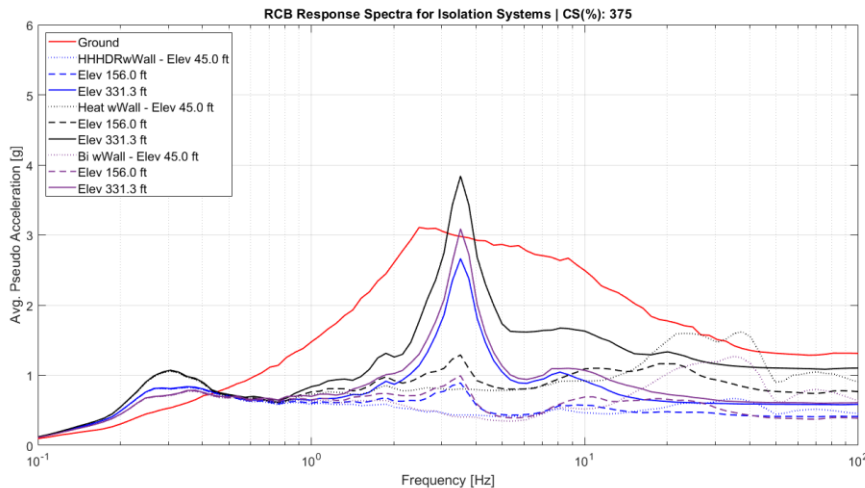


Figure 4. Floor response spectra average of 20 GMs moat wall set at CS: 375 % shear strain .

In Figure 4, the average pseudo acceleration response spectra are obtained for 20 different ground motions for three different systems: heating (LRX), the bilinear case, and the H-H-HDR system. The H-H-HDR system results in a lower response than both the upper and lower bounds by about 0.4g at 2.5 Hz, which corresponds to the fundamental frequency of the Reactor Containment Building (RCB). Also, at 8hz at the base of the RCB (45ft), the H-H-HDR model deviates substantially from the upper and lower bounds. These differences can be important if certain critical equipment is sensitive at these frequencies and therefore the other models may not capture the true response of the RCB. The differences are about 0.5g from that of the lower bound. The reason for the deviation can be due to the “Bauschinger” effect or a combination with the hardening effect. Additionally, the H-H-HDR system tends to be smoother compared to the simple Bouc-Wen (upper and lower bounds) model that may have sharper hysteresis leading to higher mode excitation.

NUMERICAL PREDICTION OF MOAT WALL POUNDING FORCE USING HIGH FIDELITY FINITE ELEMENTS

Base isolation of building structures, including nuclear power plants (NPPs), reduces earthquake-induced floor accelerations and interstory drifts by permitting large displacements at the isolation level (Christopoulos and Filiatrault 2006). During extreme ground motion events, the ground floor may exceed the provided clearance and strike the surrounding moat wall – a phenomenon known as moat wall pounding (Figure 5).

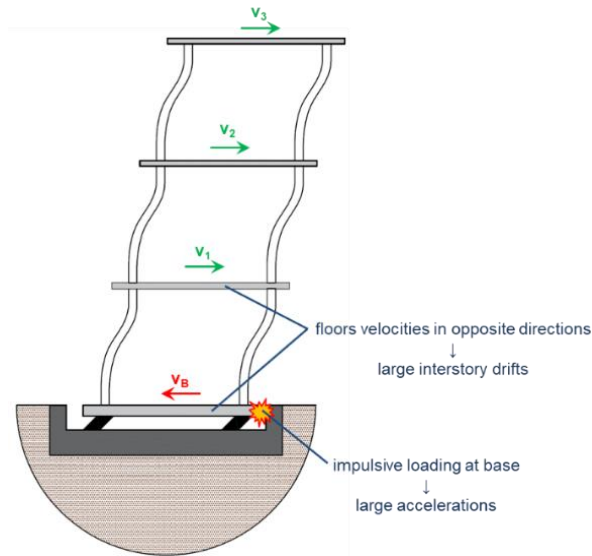


Figure 5. Amplified seismic response caused by moat wall pounding.

Studies specifically addressing moat wall pounding (Komodromos 2008, Masroor and Mosqueda, 2013, Sarebanha and Mosqueda 2017) routinely use simplified “macro” elements to predict the impact forces. While their characteristic simplicity makes macro elements amenable to large parametric studies and other repeated analyses, their reliability for a wider array of structures is not certain. Moreover, potentially significant parameters, such higher-mode vibration and wall base fixity, cannot be analyzed using macro elements.

High-fidelity finite element (FE) models, unlike macro models, must directly address all physical aspects of moat wall impact. Preliminary work by the authors (Hughes and Mosqueda 2018) showed a rough qualitative relationship between model complexity and overall impact stiffness. Essentially, detailed FE pounding models decrease in stiffness (by up to a factor of 3) as rigid connections are changed to non-rigid bolted connections. The precise mechanisms by which increased model complexity affects the pounding response is not well understood.

This section describes a moat wall pounding experiment conducted at the University at Buffalo’s Structural Engineering and Earthquake Simulation Laboratory (UB-SEESL). Following this, progress on the high-fidelity FE model of the UB-SEESL setup is presented, with a focus on the local dynamics and kinematics at the contact plane.

Description of UB-SEESL Experiments

Moat wall pounding tests at UB-SEESL involved a single-bay, three-story, base-isolated intermediate moment frame (IMF) with two different moat walls: one wedge-shaped steel wall to represent a quasi-rigid impact, and one made of reinforced concrete with sand to represent a realistic moat wall with backfill soil. The intent of this research is to calibrate a moat wall impact model against real experiment data, so further discussion is restricted to the more easily-modeled steel wall. A general schematic view and photograph of the experimental setup is shown in Figure 6. Full details of the experimental setup can be found in (Masroor and Mosqueda 2012)

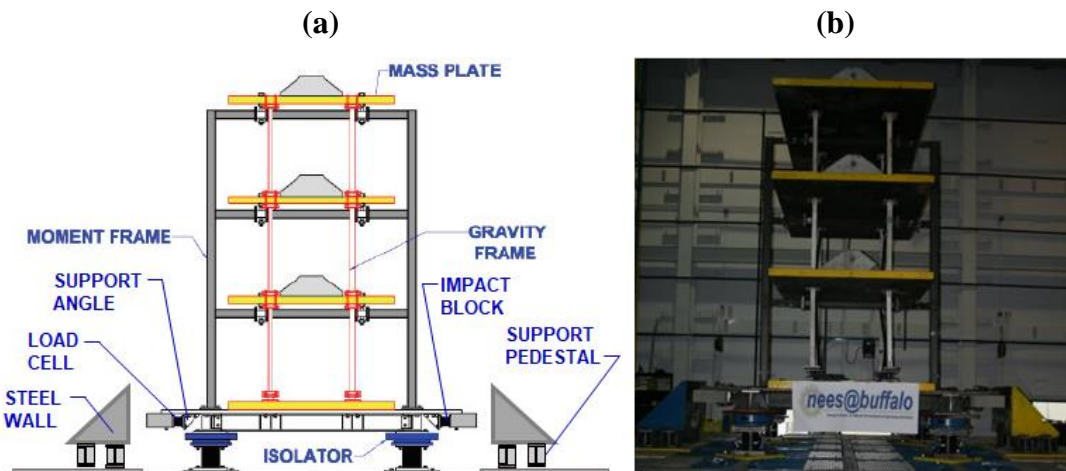


Figure 6. (a) schematic, (b) photograph of UB-SEESL moat wall pounding experiments [X].

Experimental pounding forces were measured using a special load cell sampling at 2,500 Hz. Only a single ground motion actually induced impact in the experiments: the N-S component of the 1992 earthquake in Erzincan, Turkey, scaled to the maximum credible earthquake (MCE) design level.

High-fidelity Pounding Model in LS-DYNA

The UB-SEESL experimental setup was modeled using LS-DYNA (Hallquist 2007) (see Figure 7). The base frame is given an initial relative velocity (37.2 in/sec) and collides with a stationary moat wall, and all joints are modeled with flexible bolted connections. The model consists of $\frac{1}{2}$ " cubic hexahedrons for the solid parts, and beam elements of varying cross-section for the bolts, rigid spiders, rebar, and superstructure columns. Material models are summarized in Table 2 below.

Table 2. Summary of material parameters for LS-DYNA pounding model.

Part Type	Material Model	Young's Modulus [ksi]	Poisson's Ratio	Tensile Stress [ksi]	Compressive Strength [ksi]	Unit Weight [kip/ft ³]
Steel	Bilinear w/ Kinematic Hardening	29,000	0.3	36/50/150	Same as tensile strength	495
Concrete	Winfirth	3,800	0.2	0.4	5	150

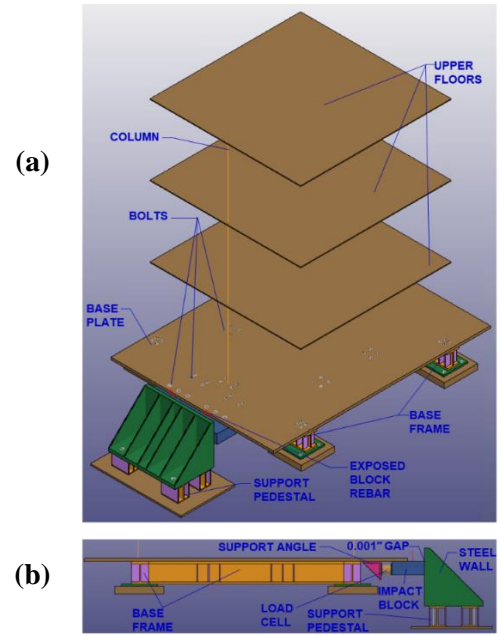


Figure 7. LS-DYNA pounding model. (a) Isometric view of entire model. (b) Close-up side view of base frame and moat wall.

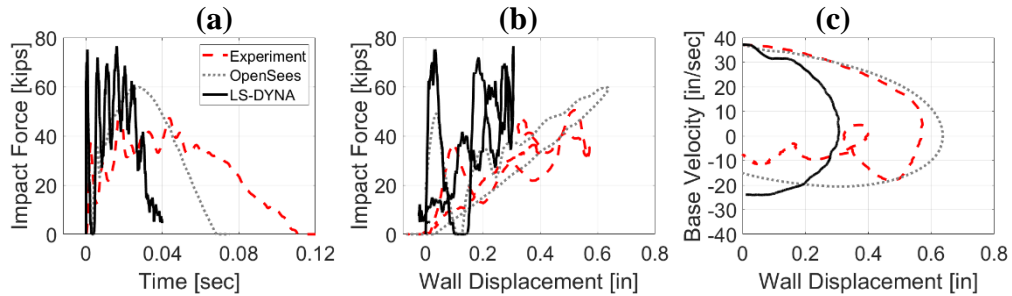


Figure 8. Impact response comparison. (a) Impact force time history, (b) impact force-displacement, (c) impact phase diagram.

Results from the explicit dynamic nonlinear time history analysis are limited to the local impact response, as the superstructure is not modeled with enough detail to consider response metrics like floor acceleration or interstory drift. Specifically, the results focus on impact force time history, impact force-displacement, and an impact phase diagram of the base plate velocity vs. moat wall displacement. Comparisons with the experimental data and Masroor element (Masroor and Mosqueda 2013) in OpenSees are shown in Figure 8.

Overall, the LS-DYNA results shown in Figure 8 represent an overly stiff model, a common problem when using solid finite elements. Peak forces are overestimated by a factor of two, and, similarly, predicted peak displacements are roughly half of those measured in the experiment. The most noticeable error is in the exit velocity, which is about three times that of the UB-SEESL experiment. Still, the LS-DYNA model provides some higher-mode vibration effects that are not captured by the OpenSees model, and the overall shape of the response curves is consistent with the experimental data. Indeed, the LS-DYNA model captures the interesting phenomenon in the force-displacement curve where the restitution force (contact force after the

base plate changes directions) is temporarily greater than the approach force (contact force before the base plate reaches zero velocity).

A normalization scheme is introduced to show how the shapes of the response curves compare, independent of their actual magnitudes. To do this, the time (t) is normalized by the entire contact duration (t_c), displacement (u) is normalized by the maximum displacement (u_{max}), force (F) is normalized by the force at maximum displacement ($F(u_{max})$), and velocity (v) is normalized by the impact velocity (v_{imp}). Normalized response curves are shown in Figure 2.4.7.

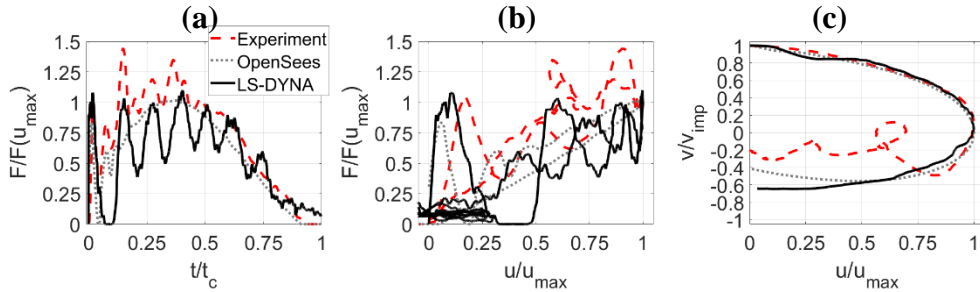


Figure 9. Normalized impact response comparison. (a) Impact force time history, (b) impact force-displacement, (c) impact phase diagram.

Figure 9 shows that, although the peak response metrics are in error, the shape of the curves match well with the experiment, including some high-frequency oscillation not captured by the Masroor element in OpenSees. This means that, in a qualitative sense, the model should be able to provide information about which of its constitutive parts control the impact response.

CONCLUSIONS

Moat wall impact, which has the potential to amplify floor accelerations and interstory drifts in base-isolated building structures, is a relatively understudied phenomenon. The best solution to mitigate the pounding effect is to extend the moat wall clearance to a distance with a low probability of exceedance by an earthquake-induced displacement at the isolation plane. For most structures, there are practical and cost constraints that limit the displacement capacity of the isolation system. In the case of nuclear power plants (NPPs), though risk precautions are taken to minimize the occurrence of impact, the avoidance of such phenomena cannot be guaranteed. As such, the possibility of impact must be studied using the best tools available: simplified macro elements and high-fidelity finite element models for the bearings and the impact interface.

A bearing model consisting of parallel components that capture the prominent nonlinear behavior observed in experimental data from testing of full-scale bearings was proposed. The use of improved models can be beneficial in better predicting the maximum displacements of the isolators and the potential for impact. Consideration of strain hardening in the rubber can be beneficial to reduce the effects of impact, especially when increasing the moat wall clearance to allow the bearing to achieve large strains to levels verified through experimental testing.

A high-fidelity finite element model of a previous moat wall pounding experiment was generated in LS-DYNA, using realistic representations of critical components. Current results show satisfactory agreement in the shape of the impact response curves, while peak forces and displacements are still in error. Future work will extend the LS-DYNA model to include a more sophisticated model of the superstructure, as well as change the simulation to a full ground motion, instead of a purely relative approach.

REFERENCES

- Bouc, R. (1967). "Forced vibration of mechanical systems with hysteresis," *4th Conference on Nonlinear Oscillations*, Prague, Czechoslovakia.
- Christopoulos, C. and Filiatraut, F. (2006). *Principles of Passive Supplemental Dampig and Seismic Isolation*. IUSS Press.
- Casciati, F. (1989). "Stochastic dynamics of hysteretic media," *Structural Safety*, 6 259-269.
- Dafalias, Y. F., Popov, E. P. (1975). "A model of nonlinearly hardening materials for complex loading," *Acta Mechanica*, 21 173-192.
- Grant, D. N., Fenves, G. L., Whittaker, A. S. (2004). Bidirectional modelling of high-damping rubber bearings. *Journal of Earthquake Engineering*, 8, 161–185.
- Huang, W. H., (2002). "Bi-directional testing, modeling, and system response of seismically isolated bridges," *PhD Thesis, University of California, Berkeley*. Berkeley, CA, USA.
- Hughes, P. J., Mosqueda, G. (2018). "Finite element analysis of moat wall pounding in base-isolated buildings," *Proceedings of the 11th U.S. National Conference on Earthquake Engineering (11NCEE)*. Los Angeles, CA, USA.
- Kalpakidis, I. V., Constantinou, M. C. (2009). "Effects of heating on the behavior of lead-rubber bearings. II: Verification of theory," *Structural Engineering*, 135, 1450–1461.
- Komodromos, P. (2008). "Simulation of the earthquake-induced pounding of seismically isolated buildings," *Computers and Structures*, 86, 618-626.
- Hallquist, J. O. (2007). "LS-DYNA keyword user's manual." *Livermore Software Technology Corporation*, 970 299-800.
- Masroor, A. and Mosqueda, G. (2012). "Experimental simulation of base-isolated buildings pounding against moat wall and effects on superstructure response," *Earthquake Engineering and Structural Dynamics*, 41 2093-2109.
- Masroor, A. and Mosqueda, G. (2013). "Impact model for simulation of base isolated buildings impacting flexible moat walls," *Earthquake Engineering and Structural Dynamics*, 42 357-376.
- McKenna F., Fenves G. L., Scott M. H. (2000). Open system for earthquake engineering simulation (OpenSees). *opensees.berkeley.edu. University of California, Berkeley*. Berkeley, CA, USA.
- Sarebanha, A. and Mosqueda, G. (2017). "Effects of moat wall impact on the seismic response of base isolated nuclear power plants," *Proceedings of the 16th World Conference on Earthquake Engineering (16WCEE)*, Santiago, Chile.
- Sarebanha, A. (2018). "Experimental and Numerical Simulation of Seismically Isolated Critical Facilities under Extreme Seismic Loading," *PhD Thesis, Univeristy of California, San Diego*. La Jolla, CA, USA.
- Schellenberg, A. H., Sarebanha, A., Schoettler, M. J., Mosqueda, G., Benzoni, G., & Mahin, S. A. (2015). "Hybrid simulation of seismic isolation systems applied to an APR-1400 nuclear power plant," *Pacific Earthquake Engineering Research (PEER) Center Report*, 5.
- Wen, Y. K. (1976). "Method for random vibration of hysteretic systems," *Journal of the Engineering Mechanic Division*, 102 249-263.
- Zhao, X. F., Zhao, Z. G., Chen, X. F., Liu, X. H., Schellenberg, A. H., Sarebanha, A., ... Robinson, W. (2015). "Hybrid simulation of seismic isolation systems applied to an APR-1400 nuclear power plant," *Corrosion and Protection*, 45 90–105.